Journal of Magnetic Resonance **146,** 58–65 (2000)
doi:10.1006/jmre.2000.2107, available online at http://www.idealibrary.com on IDEAL®

RF Pulse Concatenation for Spatially Selective Inversion

Klaas P. Pruessmann, Xavier Golay,* Matthias Stuber,† Markus B. Scheidegger, and Peter Boesiger

*Institute of Biomedical Engineering and Medical Informatics, University of Zurich and Swiss Federal Institute of Technology Zurich, CH-8092 Zurich, Switzerland; *Kennedy Krieger Institute, Johns Hopkins University, Baltimore, Maryland 21218; and †Beth Israel Deaconess Medical Center, Boston, Massachusetts 02215*

Received December 1, 1999; revised April 12, 2000

It is shown that spatially selective inversion and saturation can be achieved by concatenation of RF pulses with lower flip angles. A concatenation rule which enables global doubling of the flip angle of any given excitation pulse applied to initial *z* magnetization is proposed. In this fashion, the selectivity of the single pulse is preserved, making the high selectivity achievable in the low flip-angle regime available for inversion and large flip-angle saturation purposes. The profile quality achievable with exemplary concatenated pulses is investigated in comparison with adiabatic inversion. It is verified that by using concatenated inversion in the transfer insensitive labeling technique (TILT), the MT artifact is suppressed.

Key Words: **RF pulses; selective inversion; spin labeling; magnetization transfer; TILT.**

INTRODUCTION

The effect of RF irradiation on proton magnetization may generally be viewed as a rotation about an effective rotation axis. For MR imaging purposes, the net rotation axes of a pulse are often desired to be spatially invariant, e.g., for creating a spin echo. The design of RF pulses with this property is commonly based on Fourier principles, embedding the two transverse magnetization components in the complex plane. The complex description, however, is only a two-dimensional approximation of the essentially three-dimensional magnetization dynamics. As a consequence, the validity of the Fourier approach is limited to low flip angles. Pauly *et al.* showed that, in the low flip-angle regime, spatial invariance of the rotation axis is accomplished by pulses with Hermitian *k* space weighting along a closed trajectory (*1*). Such pulses effect pure rotations about the B_1 axis and therefore have been named inherently refocused pulses (IRP). In a following paper, the same authors extended their analysis beyond small flip angles, suggesting large flip-angle excitation by concatenation of IRPs (*2*). The composite pulse again is refocused and effects a pure B_1 rotation.

This is indeed necessary for spin-echo refocusing pulses. However, the situation is different for the inversion of *z* magnetization. Selective spin inversion is an easier task than spin-echo refocusing in that the magnetization is known to lie initially along the *z* axis. As a consequence, the net rotation axes need not be identical throughout the selected volume. Rather, for mere inversion it is sufficient to rotate longitudinal magnetization by 180° about any axes in the transverse plane.

In this paper we propose taking advantage of this freedom for creating selective inversion pulses by concatenation also of non-IRP components. It is shown that for any selective RF pulse a complementary one can be created which, if applied successively, globally doubles the net angle by which initial *z* magnetization is flipped away from the *z* axis. In this fashion, the selectivity of the single pulse is preserved, making the high selectivity achievable in the low flip-angle regime available for inversion and large flip-angle saturation purposes.

One interesting application of the proposed concept is to use concatenated 90° pulses for selective inversion in spin labeling techniques, which are widely used for perfusion imaging (*3–6*). In the labeling approach, the magnetization of arterial blood is inverted in a slab proximal to the volume of interest. As labeled blood is delivered to smaller vessels and the capillary bed, it reduces the local tissue magnetization, acting as a natural, MR detectable tracer. However, the perfusion effect on tissue magnetization is inherently weak and thus susceptible to artifacts.

In particular, spin labeling methods have long been hampered by magnetization transfer (MT) effects (*7*). The basic model of MT distinguishes two water compartments in human tissue: a free pool and a so-called bound pool of water surrounding macromolecules. Due to reduced motility, the bound pool has a very short T_2 (<100 μs). Therefore, on the one hand, it is not directly detected by MR imaging sequences. On the other hand, as a consequence of fast relaxation, the bound pool exhibits much broader absorption lines than free water protons. Therefore, in spin labeling methods the RF irradiation applied for proximal inversion affects bound water also in the volume to be imaged. Continual exchange between the two water compartments then results in net magnetization transfer from the free pool to the bound pool, reducing the magnetization of free water. In this fashion, MT mimics the perfusion effect and results in perfusion overestimation.

The MT effect as such is an inevitable response to labeling RF irradiation. However, in labeling subtraction schemes it can be compensated for, as first proposed by Detre *et al.* in their

1090-7807/00 $35.00

original paper (*3*). Using flow-driven, continuous inversion, they suggested additional distal labeling during control preparation in order to have MT effects cancel out in image subtraction. Later, the distal control approach was also used in the pulsed spin labeling technique EPISTAR (echo-planar imaging and signal targeting with alternating radiofrequency) (*6*). However, there are two major drawbacks to distal labeling as a compensation mechanism. First, for exact MT correction it requires mirror symmetry of the proximal and distal selections about the imaged volume and thus restricts imaging to one slice. Second, with distal labeling for control, potential distal inflow may give rise to perfusion misjudgment.

For continuous labeling, Alsop and co-workers recently suggested an alternative control strategy (*8*), which does not rely on distal RF power deposition. Instead, during control preparation, RF is deposited by rotating the magnetization of proximally inflowing blood by 360°. Double inversion is elegantly accomplished by cosine modulation of the RF envelope, splitting the RF into two frequency components, corresponding to two inversion planes. Yet, this solution makes specific use of flow-driven, adiabatic excitation and thus is not applicable in pulsed methods.

For MT-compensated perfusion imaging with pulsed RF, recently the transfer insensitive labeling technique (TILT) was proposed (*9, 10*). Using pulse concatenation for labeling, this technique was designed to globally compensate for MT without geometric restriction of imaging or distal labeling. The experimental evaluation of labeling by concatenated pulses forms the second focus of the present paper. Profile quality and MT compensation as achieved with TILT were studied by means of numerical simulations and phantom experiments.

THEORY AND METHODS

Doubling the Flip Angle by a Complementary Pulse

For any spatially selective RF and gradient sequence S_1, a complementary one exists, which, if applied successively, globally doubles the net angle by which initial z magnetization is flipped away from the z axis. The complementary sequence can be derived from the reverse of the original. The latter is obtained by inverting S_1 in time, changing the sign of the gradient and frequency modulation (FM) waveforms, and shifting the RF phase by 180°. Here as frequency modulation we consider the frequency offset with respect to the Larmor frequency in the isocenter where the gradient fields do not contribute to the net field. In the absence of relaxation and additional frequency offsets, the reverse ideally rewinds the rotation performed by S_1 when applied successively. The complementary counterpart of S_1 is identical to the reverse except for the phase shift. For creating the complement, the phase of the original RF pulse is preserved.

To prove flip-angle doubling, consider a general excitation sequence S_1 of duration T. Neglecting relaxation, the Bloch equation describing the effect of S_1 at a given location can be expressed in terms of the rotation matrix $R_1(t)$,

$$\frac{d}{dt}R_1(t) = A_1(t)\,R_1(t), \quad R_1(0) = \mathrm{Id} \qquad [1]$$

with

$$A_1(t) = \gamma\begin{pmatrix} 0 & B_z(t) & -B_y(t) \\ -B_z(t) & 0 & B_x(t) \\ B_y(t) & -B_x(t) & 0 \end{pmatrix}, \qquad [2]$$

where Id denotes 3×3 identity, γ is the gyromagnetic ratio of protons, and B_x, B_y, and B_z are the components of the time-dependent net magnetic field. The rotation resulting from S_1 is denoted

$$\hat{R}_1 = R_1(T). \qquad [3]$$

According to the rule given above, the Bloch equation for the complementary sequence, S_2, is identical to Eq. [1], except for time inversion and changing of the sign of B_z. Using the mirror transform

$$U = \begin{pmatrix} +1 & 0 & 0 \\ 0 & +1 & 0 \\ 0 & 0 & -1 \end{pmatrix}, \qquad [4]$$

it reads

$$\frac{d}{dt}R_2(t) = -UA_1(T-t)U^{-1}R_2(t), \quad R_2(0) = \mathrm{Id}, \qquad [5]$$

with the solution

$$R_2(t) = UR_1(T-t)\hat{R}_1^{-1}U^{-1}. \qquad [6]$$

Hence, the rotation through S_2 is given by

$$\hat{R}_2 = R_2(T) = U\hat{R}_1^{-1}U^{-1}. \qquad [7]$$

The net flip angles φ_1, $\varphi_{21,}$ as effected by applying S_1 and the concatenation S_2S_1, respectively, to z magnetization, are given by

$$\cos(\varphi_1) = z^{\mathrm{T}}\hat{R}_1 z, \qquad [8]$$

$$\cos(\varphi_{21}) = z^{\mathrm{T}}\hat{R}_2\hat{R}_1 z, \qquad [9]$$

where z denotes the unit vector in the z direction.

For explicit calculation of the cosine terms, we choose a frame of reference in which the rotation axis of $\hat{R}_1$ lies in the

y–z plane. Let α denote the rotation angle of $\hat{R}_1$ and θ the angle between its rotation axis and the z axis. Then $\hat{R}_1$ is given by

$$\hat{R}_1 = \begin{pmatrix} 1 & 0 & 0 \\ 0 & \cos\theta & -\sin\theta \\ 0 & \sin\theta & \cos\theta \end{pmatrix} \begin{pmatrix} \cos\alpha & -\sin\alpha & 0 \\ \sin\alpha & \cos\alpha & 0 \\ 0 & 0 & 1 \end{pmatrix} \times \begin{pmatrix} 1 & 0 & 0 \\ 0 & \cos\theta & \sin\theta \\ 0 & -\sin\theta & \cos\theta \end{pmatrix}. \quad [10]$$

The evaluation of Eqs. [8] and [9], using Eqs. [7] and [10], yields

$$\cos(\varphi_1) = \cos^2(\theta) + \cos(\alpha)\sin^2(\theta) \quad [11]$$

$$\cos(\varphi_{21}) = (\cos^2(\theta) + \cos(\alpha)\sin^2(\theta))^2 - \sin^2(\alpha)\sin^2(\theta) - \sin^4\left(\frac{\alpha}{2}\right)\sin^2(2\theta). \quad [12]$$

By substitution of Eq. [11] into the right-hand side of the identity

$$\cos(2\varphi_1) = 2\cos^2(\varphi_1) - 1 \quad [13]$$

we obtain

$$\cos(2\varphi_1) = 2(\cos^2(\theta) + \cos(\alpha)\sin^2(\theta))^2 - 1. \quad [14]$$

Common trigonometric transformation yields that the right-hand sides of Eqs. [12] and [14] are equal. Hence

$$2\varphi_1 = \varphi_{21}. \quad [15]$$

This holds independently at any position. Thus, the net flip angle of any excitation sequence applied to z magnetization is globally doubled by concatenation with its complementary sequence.

The rotation axis belonging to $\hat{R}_1$, $\mathbf{a}_1$, is characterized by the fact that it remains unchanged when rotated by $\hat{R}_1$:

$$\hat{R}_1\mathbf{a}_1 = \mathbf{a}_1. \quad [16]$$

Similarly, according to Eq. [7], the rotation axis of $\hat{R}_2$, $\mathbf{a}_2$, is described by

$$U\hat{R}_1^{-1}U^{-1}\mathbf{a}_2 = \mathbf{a}_2, \quad [17]$$

which is solved by

$$\mathbf{a}_2 = U\mathbf{a}_1. \quad [18]$$

Hence the second rotation axis is a copy of the first, mirrored about the transverse plane. Due to this symmetry, the net rotation axis, which results from the successive application of the two sequences, always lies in the transverse plane. Therefore, once doubled, the flip angle can be further multiplied by simply iterating the composite sequence. Note that due to the symmetry induced by the concatenation rule, the complementary counterpart of a composite pulse is identical to the composite pulse itself. Thus, playing out a composite pulse multiple times is equivalent to iterating the concatenation process starting from the composite pulse. This corresponds to the fact that when $\mathbf{a}_1$ is transverse already, it has an identical mirrored counterpart $\mathbf{a}_2$.

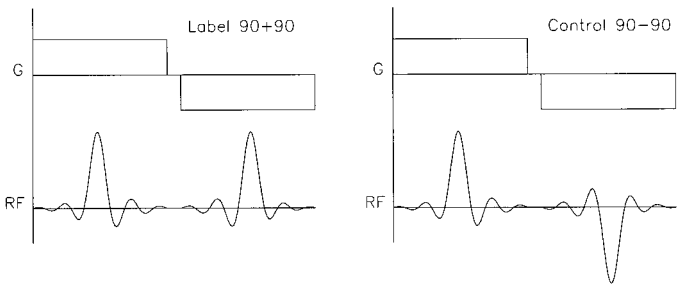

FIG. 1. Sequence elements of the TILT scheme. (Left) Labeling is achieved by concatenation of two selective 90° pulses. The selection gradients (G) have opposite polarity and the second RF envelope is inverted in time. (Right) For control preparation the phase of the second RF portion is shifted by 180°. In this fashion the second pulse is made the inverse of the first one and has a rewinding effect.

The concatenation rule ensures only that the resulting net rotation axes are transverse, while no general statements can be made about their relative angles. In the general case, the net rotation axes are not aligned and not refocusable by linear gradient fields. For this reason, the concept is strictly applicable only when the relative phases of resulting transverse magnetization are not of interest. This is true for inversion and saturation purposes, while coherent excitation and refocusing do require well-defined phase relations.

Transfer Insensitive Labeling

In the TILT method, the proposed concatenation concept is used for the purpose of eliminating the MT artifact. Figure 1 shows schematic representations of the pulse combinations used in TILT for labeling and control preparation. Spin labeling is performed by concatenating a selective 90° pulse with its complementary counterpart. Both pulses are applied at constant frequency. For selecting a slice off the isocenter, the first pulse is applied with a frequency offset. For the second pulse such offset is inverted according to the concatenation rule.

For control preparation, the phase of the second pulse is shifted by 180°. According to the definition of the complementary sequence, this phase shift makes the second pulse the reverse of the first. Thus, in control preparation the magnetization is first selectively flipped by 90° and then rewound, resulting in the desired control state with no labeling. In this fashion, shifting the phase of the second RF pulse permits

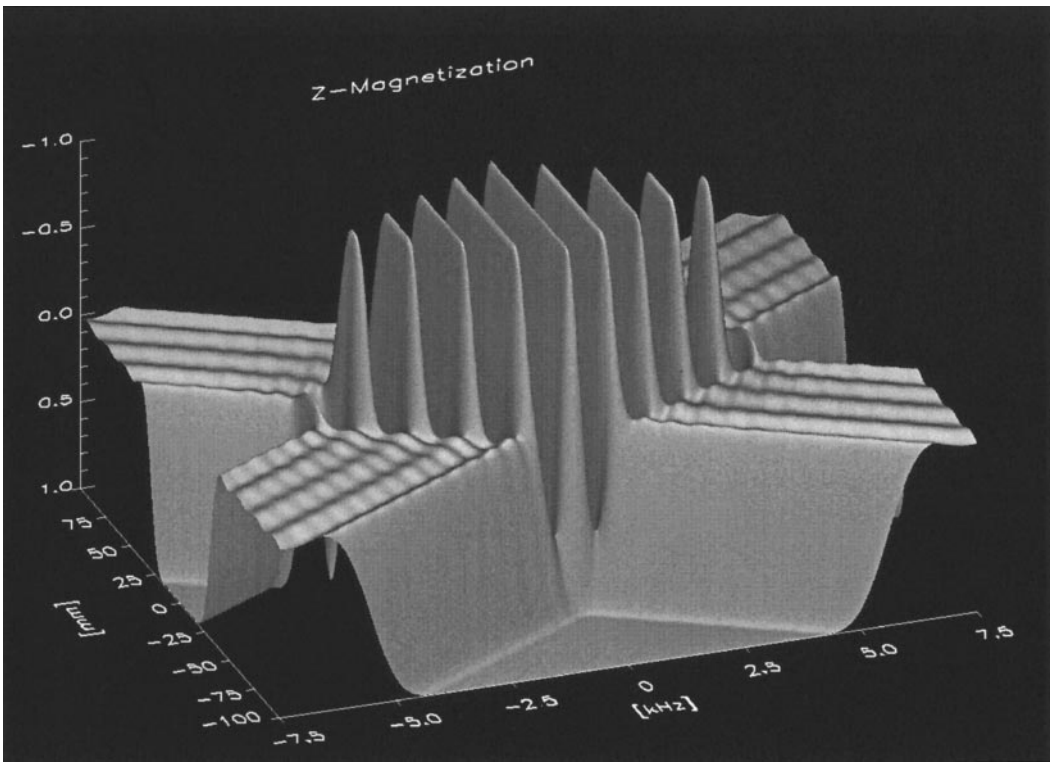

FIG. 2. Spectral dependence of the inversion profile obtained with concatenated 90° pulses (Fig. 1, left). The RF effect on unit magnetization was simulated by solving the Bloch equation with exemplary pulse duration of 1 ms each. The resulting *z* magnetization is plotted against frequency offset (left–right) and spatial selection direction (front–back). The component pulses interact only in the intersection of tilted selection bands. Within the interaction zone, the inversion profile shows a periodic spectral dependence related to wrapping of the offset phase accumulated between the two RF amplitude peaks.

switching between labeling and control preparation. In particular, the two preparation modes differ only in the phase of the second pulse.

MT compensation in TILT is based on the T_2 difference between free water and the bound pool. Note that both doubling the flip angle and rewinding the magnetization rely on the negligibility of relaxation during and between the component pulses. This assumption usually holds well for free water where T_2 is significantly longer than typical pulse durations. However, in the bound pool with much shorter T_2, the situation is different. Due to fast transverse relaxation, the magnetization vector of bound water is only a little flipped away from the *z* axis during RF irradiation. The main effect of RF on bound water magnetization is a gradual reduction of the longitudinal component. Furthermore, in labeling as well as control preparation, a short break between the RF portions is naturally induced by the need to switch the selection gradient. During this break of typically several hundred microseconds, bound water undergoes virtually complete transverse relaxation. In other words, bound water magnetization loses any phase information related to the first pulse. Therefore, it does not sense the RF phase shift used to switch between labeling and control preparation. As a consequence, both ways of preparation alter bound water *z* magnetization in virtually exactly the same way throughout the object. In this fashion, magnetization transfer effects are globally canceled out upon image subtraction, making TILT imaging insensitive to MT.

Influence of Frequency Offsets

In creating the complementary counterpart of a pulse, the inversion of the gradient and FM waveforms has a crucial role. The resulting mirror symmetry of the effective magnetic field about the transverse plane underlies the doubling of the flip angle of the single pulse. For the strict validity of Eq. [5] it is necessary that variations of the Larmor frequency in the sample indeed arise only from switchable external gradients. Additional frequency offsets due to chemical shift and B_0 inhomogeneity cannot be inverted for the complementary pulse and thus violate the assumed symmetry.

Practically, frequency offsets that are not inverted lead to destructive coaction of the two RF portions when the offset phase accumulated between the pulse centers is an odd multiple of 180°. As a consequence, the resulting excitation profile exhibits a periodic dependence on the frequency offset. This is illustrated by Fig. 2, showing qualitatively the spectral dependence of *z* magnetization as resulting from the labeling sequence sketched in Fig. 1. The periodic spectral dependence observed in the center of the plot is typical for pulse trains with alternating gradient lobes as also used, e.g., for spectral–spatial

selective excitation (*11*). The spectral distance of neighboring peaks is the inverse of the time between the amplitude peaks of successive RF pulses in the pulse train. The width of the frequency selection band is the inverse of the time interval between the first and last RF amplitude peaks.

In addition to phase effects, frequency offsets result in spatial shifts of the selected volume. Due to the inversion of gradients and FM for the second part of a concatenation, the sensitive volume is shifted in opposite directions for the two RF portions. As seen in Fig. 2, in a spectral–spatial plot the sensitive volumes of the two pulses form tilted bands. The slope of these bands is characterized by the strength of the selection gradients. Pulse coaction is restricted to the central intersection of these bands where both pulses have an effect.

EXPERIMENTS AND RESULTS

Experimental evaluations were performed on a 1.5-T Philips Gyroscan ACS-NT whole-body MR system (Philips Medical Systems, Best, The Netherlands). TILT labeling and control preparation sequences, as depicted in Fig. 1, were created using an asymmetrical 90° pulse, which is a numerically optimized variant of a Gauss-windowed sinc shape with four full side lobes. The pulse shape is drawn to scale in Fig. 1, while the gradient lobes and the time gap between the pulses are represented only schematically. The duration of a single RF portion was 2.2 ms, with a bandwidth of 4.59 kHz. The gap between the pulses was 1.0 ms, resulting in the full duration of 5.4 ms for each sequence.

For comparison, all labeling experiments were repeated using standard hyperbolic secant (HS) AFP pulses with virtual angles $\alpha = 600°$, 1000°, and 2000°, where by "virtual angle" we denote

$$\alpha = \int \gamma B_1(t)dt. \qquad [19]$$

The AFP pulses were realized with a maximum B_1 of 20 μT, resulting in pulse durations of 6.4, 10.6, and 21.2 ms, respectively. Simulations were carried out by numerical integration of the Bloch equations with relaxation taken into account. The quality of labeling profiles in free water was studied by experiments on a water phantom. The phantom was doped with 30 mg/liter $MnSO_4$, resulting in relaxation times $T_1 = 655$ ms and $T_2 = 97$ ms (at 1.5 T), which are in the same range as those present in brain tissue. TILT labeling was used for inversion of a 100-mm-thick slab in an inversion-recovery spin-echo sequence with readout parallel to the inversion gradient ($G = 1.08$ mT/m). The delay between inversion and imaging was varied in eight steps from 50 to 1000 ms. In this fashion, a series of slice profiles with increasing T_1 relaxation effect was obtained, enabling the determination of the state of the z magnetization immediately after excitation by exponential fitting. Using the same procedure, slice profiles were also created for TILT control preparation and AFP labeling.

The resulting slice profiles are shown in Fig. 3, with simulation results added for comparison. It is seen that the concatenation of two 90° pulses indeed acts as an inversion pulse, while in TILT control preparation the magnetization is rewound by the second pulse. In terms of overall selectivity, the profile of the concatenated sinc–Gauss inversion is comparable to that of the 1000° AFP pulse. However, in the experimental TILT profile a slight reduction of absolute z magnetization is observed, which deviates from the simulation. This discrepancy is due to microscopic field inhomogeneities, which affect TILT labeling due to its sensitivity to frequency offsets.

Figure 4 shows the tails of the simulated labeling profiles shown in Fig. 3 in a close-up view. It is seen that in terms of out-of-slice contamination the concatenated sinc–Gauss inversion is theoretically superior to the AFP pulses. Additional simulations with relaxation ignored revealed that there are two different reasons for the more marked tails obtained with common AFP labeling. With the 600° pulse, the selectivity is mainly limited by the violation of the adiabatic condition at slab edges. With increasing pulse duration, profile broadening due to relaxation becomes more significant and is the dominant reason for the contamination obtained with the 2000° AFP pulse.

A second series of phantom experiments focused on the MT effect. On the one hand, the suppression of the MT artifact in TILT was to be verified. On the other hand, the potential artifact in labeling data without MT compensation was to be demonstrated. For this purpose, a phantom consisting of two bottles was used (Fig. 5). One bottle was filled with agar gel (8%), exhibiting a relatively large bound water pool. The second bottle was filled with water for reference. TILT labeling and control images were obtained from a 10-mm slice. The gap between the imaged slice and the 100-mm-thick labeling slab was varied between 0 and 10 cm by shifting the latter. For imaging a common gradient-echo sequence was used. The delay between labeling and imaging was $T_I = 500$ ms, and the repetition time was $T_R = 5000$ ms. To demonstrate the MT artifact, the same procedure was repeated with AFP labeling and no control preparation.

To quantify the MT effect in the agar gel, a region of interest (ROI) was selected inside each phantom bottle in the image plane. Individual image scaling by the scanner software was compensated for by scaling all images such as to yield unit mean modulus in the water ROI where no MT was present. Then the relative MT artifact was determined by subtracting the mean modulus values in the agar ROI of corresponding labeling and control images and dividing the difference by the control value:

$$\mathrm{MT} = \frac{\mathrm{Avg}[|\mathrm{Control}|] - \mathrm{Avg}[|\mathrm{Label}|]}{\mathrm{Avg}[|\mathrm{Control}|]}. \qquad [20]$$

The resulting artifact percentages are shown in Fig. 6. Consid-

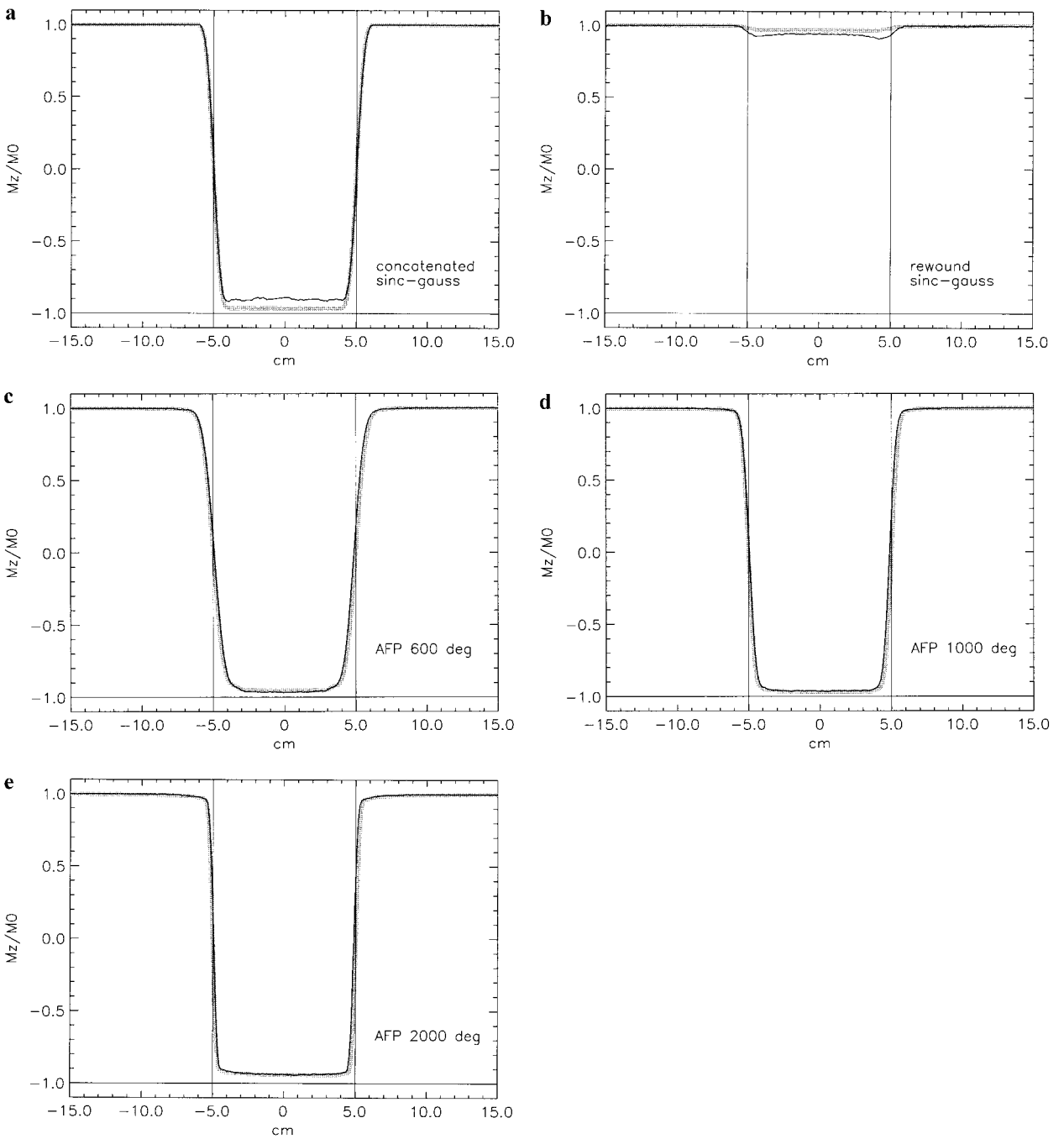

FIG. 3. Selection profiles obtained with TILT preparation sequences (a, b) and AFP pulses (c, d, e). Relative z magnetization as resulting immediately after application of the pulse is plotted against position. Thin black lines show experimental results, and thick gray lines show simulated profiles for verification. The nominal width of the selection is 10.0 cm, the limits being indicated by vertical lines. The relaxation times were $T_1 = 655$ ms and $T_2 = 97$ ms (1.5 T).

erable MT effects are evident in the data obtained with AFP labeling. In agreement with MT theory, the effect increases with the virtual pulse angle and decreases with the distance from the labeling slab. The reduced and partly negative artifact values at small distances reflect the imperfections of the slice profiles where free water magnetization was directly saturated by labeling RF. The effect of direct saturation has the opposite sign of the MT effect due to the initial scaling according to the water ROI. Where free water is directly saturated, the scaling step results in signal overestimation in the labeling images. Thereby the saturation effect in the agar is overcompensated since T_1 relaxation in water is much slower. In this fashion, the slice profile effects are clearly distinguished from MT. In agreement with the simulations, the 600° AFP profile exhibits the strongest slice profile effect, while with 1000° and 2000° AFP pulses the slice tails gradually become less prominent.

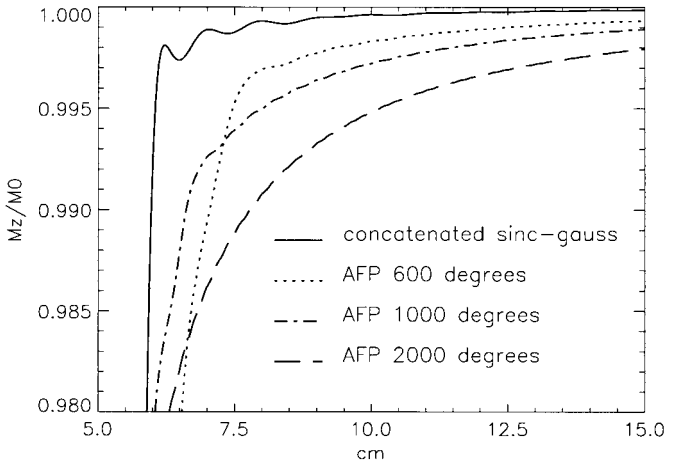

FIG. 4. Close-up view of the simulated labeling profiles shown in Fig. 2. The right tails are plotted from the nominal slab limit. Note the vertical scale. With TILT labeling, contamination drops sharply at a distance of 1 cm from the labeling slab. The tails of the AFP profiles are due to violation of the adiabatic condition (600°, 1000°) and to relaxation effects (1000°, 2000°).

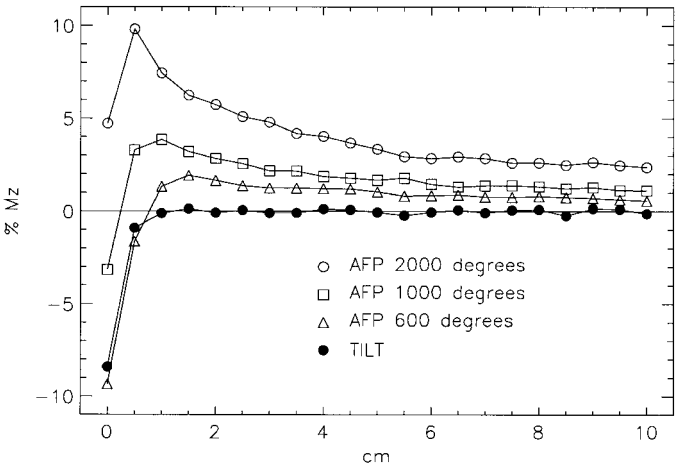

FIG. 6. Signal changes in agar gel due to labeling, as assessed in subtraction images obtained with TILT and AFP labeling. The percentage of M_z reduction due to labeling is plotted against the gap width between labeling slab and imaging slice. Considerable MT artifact is obtained with AFP inversion, while transfer effects are compensated with TILT. Near the labeling slab, slice profile effects are observed, having the opposite of the MT effect due to calibration with a water reference.

Slice imperfection is also observed in the TILT data. However, at distances of 10 mm and more, no significant artifact is found, indicating that MT effects were indeed successfully suppressed.

DISCUSSION

The concatenation principle proposed in this work generally permits doubling the flip angle of any RF pulse when applied to *z* magnetization. The inversion profile obtained by an exemplary pulse pair has been evaluated in comparison with that achieved with HS-AFP pulses as commonly used in arterial labeling techniques. It has been demonstrated that pulse concatenation enables inversion with a profile quality similar to that achievable with common, 1000° HS-AFP. Generally, the concatenation concept enables fairly high profile quality at short pulse duration and low RF deposition. For sharpest inversion profiles, however, the adiabatic principle clearly is more appropriate. In particular, advanced variants like FOCI pulses (*12*, *13*) yield a superior profile quality that cannot be matched by concatenation of non-frequency-modulated pulses. With respect to the pulse combination used in this work, some profile improvements shall be possible by further numerical optimization of the component pulses, using, e.g., the SLR approach (*14*, *15*) or iterative optimization. Note that the numerical generation of 90° pulses usually aims at coherence of transverse magnetization along with profile quality. However, refocusing of the transverse component is not required for concatenation components. The added freedom may facilitate the numerical determination of improved component pulses.

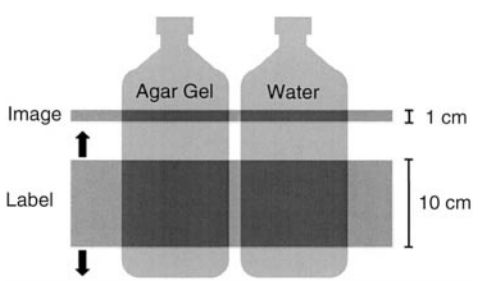

FIG. 5. Experimental verification of the insensitivity of TILT labeling to magnetization transfer (MT), using an agar phantom and water as reference. Magnetization was inverted in a 10-cm-thick labeling slab. After a delay of 500 ms, MT-related signal reduction was assessed by imaging of a 1-cm-thick slice at varying distance from the labeled volume.

In principle, the concatenation concept holds for any combination of RF amplitude, FM, and gradient waveforms, including adiabatic pulses. In concatenations of adiabatic pulses, care must be taken that the adiabatic condition is not violated by the required zero crossings of gradients and FM. Besides this restriction, concatenating adiabatic pulses for the purpose of selective inversion generally seems little useful. On the one hand, spatially selective adiabatic excitation with low flip angles up to 90° is not straightforward. At the same time, excellent inversion selectivity is available with relatively basic waveforms. In this sense, the problems of the adiabatic approach are opposite to those faced with non-frequency-modulated pulses. On the other hand, adiabatic pulses tend to require longer pulse durations, causing more marked relaxation effects in violation of the assumptions made in the concatenation approach. Nevertheless, the arguments used in this work may be of some use for theoretical considerations of adiabatic pulses, as many species of adiabatic pulses exhibit symmetries similar to those induced by the concatenation rule.

It has been shown that the concatenation of a pulse with its complementary counterpart globally ensures transverse net ro-

tation axes. Therefore, such concatenations can theoretically be iterated for the purpose of flipping magnetization away from the *z* axis. This kind of iteration is similar to the concatenation of IRPs with canceling rephase and prephase gradient lobes, as suggested by Pauly *et al.* (*16*). However, the arguments used in this work also hold for non-IRP components. Therefore, asymmetric RF envelopes can be used and the component pulses need not directly fulfill the low flip-angle assumption.

A common property of RF pulse trains with switched selection gradients is the spectral dependence of the selection profile (*11*). It has been found that frequency offsets due to field inhomogeneity reduce the net flip angle resulting from the concatenation of two 90° pulses. The spectral inversion bandwidth is inversely proportional to the peak-to-peak interval of the concatenated RF portions. Therefore, to minimize the spectral dependence of the inversion profile, the maximal available B_1 power and gradient switching rate should be used. Non-IRP concatenation of two RF pulses, as used in this work, offers a further means of increasing the selection band. In this case, the RF peak-to-peak interval can further be reduced by using asymmetrical RF envelopes with a noncentered main lobe. Finally, for concatenated pulses just as for spectral–spatial excitation, the spectral bandwidth present in the sample should be narrowed as much as possible by shimming.

The concatenation concept proposed in this work is of particular interest for spin labeling as it offers a straightforward solution of the MT problem. It has been found that, using concatenated labeling in the TILT scheme, magnetization transfer is indeed globally compensated for. As opposed to control concepts based on distal labeling, the method does not impose any geometric restrictions on the imaging volume. Furthermore, unlike techniques with distal control, TILT perfusion mapping is not prone to errors due to distal inflow during control imaging. From the spatial variation of the MT effect, as observed in the agar phantom, it is also conceivable that distal control indeed requires approximate mirror symmetry for reliable MT compensation.

Recently, Norris independently developed a similar method for MT compensation in perfusion imaging (*17*). The approach described in that work is based on the decomposition of a symmetrical inversion pulse into the two parts induced by symmetry. As opposed to that, in TILT two 90° pulses are concatenated for net inversion. The two techniques furthermore differ in the way the selection gradients are switched. Unlike TILT, in Norris' method the selection gradient is switched only during control preparation while during labeling its polarity is maintained. Therefore, to ensure MT equivalence of the two preparation sequences, the method requires the absorption spectrum of the bound water pool to be symmetrical (*17*). In principle, this assumption does not strictly hold when field inhomogeneities induce shifts in the bound water spectrum. However, the effect of field inhomogeneity is usually small with respect to the bandwidth of the bound water absorption line. On the other hand, the constant labeling gradient in Norris' method certainly has the advantage of making labeling more robust against frequency offsets in the free water pool.

REFERENCES

1. J. Pauly, D. Nishimura, and A. Macovski, A *k*-space analysis of small-tip-angle excitation, *J. Magn. Reson.* **81,** 43–56 (1989).
2. J. Pauly, D. Nishimura, and A. Macovski, A linear class of large-tip-angle selective excitation pulses, *J. Magn. Reson.* **82,** 571–587 (1989).
3. J. A. Detre, J. S. Leigh, D. S. Williams, and A. P. Koretsky, Perfusion imaging, *Magn. Reson. Med.* **23,** 37–45 (1992).
4. S. G. Kim, Quantification of regional cerebral blood flow change by flow sensitive alternating inversion recovery (FAIR) technique: Application to functional mapping, *Magn. Reson. Med.* **34,** 293–301 (1995).
5. K. K. Kwong, D. A. Chesler, R. M. Weisskoff, K. M. Donahue, T. L. Davis, L. Ostergaard, T. A. Campbell, and B. R. Rosen, MR perfusion studies with T1-weighted echo planar imaging, *Magn. Reson. Med.* **34,** 878–887 (1995).
6. R. R. Edelman, B. Siewert, D. G. Darby, V. Thangaraj, A. C. Nobre, M. M. Mesulam, and S. Warach, Qualitative mapping of cerebral blood flow and functional localization with echo-planar MR imaging and signal targeting with alternating radio frequency, *Radiology* **192,** 513–520 (1994).
7. S. D. Wolff and R. S. Balaban, Magnetization transfer contrast (MTC) and tissue water proton relaxation in vivo, *Magn. Reson. Med.* **10,** 135–144 (1989).
8. D. C. Alsop, L. Maccotta, and J. A. Detre, Multi-slice perfusion imaging using adiabatic arterial spin labeling and an amplitude modulated control, *in* "Proceedings, ISMRM, 5th Annual Meeting, Vancouver," p. 81 (1997).
9. K. P. Pruessmann, X. Golay, M. Stuber, M. B. Scheidegger, and P. Boesiger, Transfer insensitive labeling for 3D MR perfusion assessment, *NeuroImage* **7,** S535 (1998).
10. X. Golay, M. Stuber, K. P. Pruessmann, D. Meier, and P. Boesiger, Transfer insensitive labeling technique (TILT): Application to multislice functional perfusion imaging, *J. Magn. Reson. Imaging* **9,** 454–461 (1999).
11. C. H. Meyer, J. M. Pauly, A. Macovski, and D. G. Nishimura, Simultaneous spatial and spectral selective excitation, *Magn. Reson. Med.* **15,** 287–304 (1990).
12. S. Connoly, D. Nishimura, and A. Macovski, Variable rate selective excitation, *J. Magn. Reson.* **78,** 440–458 (1988).
13. R. J. Ordidge, M. Wylezinska, J. W. Hugg, E. Butterworth, and F. Franconi, Frequency offset corrected inversion (FOCI) pulses for use in localized spectroscopy, *Magn. Reson. Med.* **36,** 562–566 (1996).
14. M. Shinnar, L. Bolinger, and J. S. Leigh, *in* "Proceedings, Seventh Annual Meeting of the Society of Magnetic Resonance in Medicine," p. 659, (1988).
15. P. Le Roux, Abstracts of the Society of Magnetic Resonance in Medicine, 7th Annual Meeting, p. 1049 (1988).
16. J. Pauly, D. Spielman, and A. Macovski, Echo-planar spin-echo and inversion pulses, *Magn. Reson. Med.* **29,** 776–782 (1993).
17. D. G. Norris, 0° slice-selective RF pulses: MT-equivalence for multislice perfusion imaging, *in* "Proceedings, ISMRM, 6th Annual Meeting, Sydney," p. 1211 (1998).